JACS Au
AN OPEN ACCESS JOURNAL OF THE AMERICAN CHEMICAL SOCIETY

pubs.acs.org/jacsau
Article

Total Synthesis of Altemicidin: A Surprise Ending for a Monoterpene Alkaloid

Claire S. Harmange Magnani, José R. Hernández-Meléndez, Dean J. Tantillo, and Thomas J. Maimone*

Cite This: JACS Au 2023, 3, 2883−2893
Read Online

ACCESS | Metrics & More | Article Recommendations | Supporting Information

ABSTRACT: Monoterpene alkaloids encompass distinct chemical diversity and wide-ranging bioactivity. Their compact complexity has made them popular as synthetic targets and has inspired many distinct strategies and tactics in the field of heterocyclic chemistry. This article documents the evolution of a synthetic program aimed at accessing the unusual sulfonamide-containing natural product altemicidin, which was generally believed to be a monoterpene alkaloid throughout our entire synthetic investigations but has recently been found to originate through an unexpected and quite disparate biosynthetic pathway. By leveraging a pyridine dearomatization/cycloaddition strategy, we developed a concise pathway to the 5,6-fused bicyclic azaindane core and, after significant experimentation, an ultimate synthesis of altemicidin itself. Tactics to productively manipulate the multiple functional groups present on this highly polar scaffold proved challenging but were eventually realized via several carefully orchestrated and chemoselective transformations—investments that paid dividends in the form of significantly shorter chemical synthesis. Surprisingly, the bond-forming logic between our presumed abiotic synthetic strategy to this alkaloid class and its subsequently identified biosynthetic pathway is eerily similar.

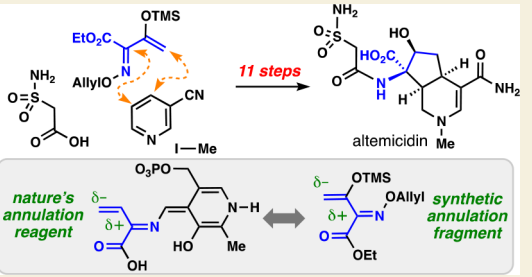

KEYWORDS: *alkaloid, total synthesis, biosynthesis, cycloaddition, pyridine, dearomatization, heterocyclic chemistry*

INTRODUCTION

Altemicidin (**1**) and its related family members, (+)-SB-203207 (**2**) and (+)-SB-203208 (**3**), are alkaloid natural products produced by *Streptomyces* bacteria (Figure 1A).[1−3] First isolated in 1989, **1** showed promising antitumor activity against L1210 lymphocytic leukemia and IMC carcinoma cell lines with IC50s of 0.84 and 0.82 μg/mL, respectively. Derivatives **2** and **3** were later discovered by researchers at SmithKline Beecham pharmaceuticals from a different *Streptomyces* strain (*sp. NCIMB*).[4] These compounds were characterized as potent tRNA synthetase inhibitors. SB-203208 (**2**) demonstrated low nanomolar (1.4 to 1.7 nM) inhibitory activity against tRNA synthetases isolated from *Staphylococcus aureus, Pseudomonas fluorescens*, and *Candida albicans*. It is believed that **2** and **3** mimic naturally occurring substrates processed by tRNA synthetases, namely isoleucyl adenosine monophosphate (Ile-AMP) in the case of isoleucine tRNA synthetase inhibitory activity exhibited by **2**. Further studies revealed that changing the identity of the amino acid appended to **1** (Val and Leu) could also engender inhibitory activity toward the corresponding synthetase for that amino acid.[5,6]

Alkaloids **1**-**3** all share a characteristic 5,6-*cis*-fused azaindane bicycle, α,α-quaternary-α-amino stereocenter, and rare sulfonamide side chain.[7] Abe and co-workers have shown that this sulfonamide side chain is biosynthesized from *L*-cysteine through a series of oxidations mediated by iron(II)-containing enzymes, with resemblance to cupin-type cysteine dioxygenases.[8] These researchers further demonstrated that altemicidin is a substrate of aminoacyl transfer enzymes SbzA and SbzC, which append the isoleucine (shown in green) and β-methyl-phenylalanine (shown in orange) side chains, respectively. At the start of our work in 2017, and throughout our entire synthetic journey to **1**, the biosynthesis of the azaindane core of **1**−**3** had not been reported, yet all literature reports logically classified these compounds as monoterpenoid alkaloids. Monoterpene alkaloids comprise several hundred members (see Figure 1B for representative examples), and are typically produced by plants, not bacteria.[9] Originating from the iridoid-loganin biosynthetic pathway, all family members harbor a distinctive 5,6-fused bicyclic ring system with piperidine (see **4**-**10**) or pyridine (see **11**) heterocycles. Many possess desaturation patterns similar to those of **1**-**3**, including dinklageine (**4**), nepetalactam (**5**), and lindenialine (**6**), and varying stereochemistry patterns are noted at the 5,6 ring fusion (see protons in red, Figure 1B). Additionally, hydroxylation is noted on the cyclopentane ring at precisely the same positions as needed for the biosynthesis of **1**−**3**.

Received: July 28, 2023
Revised: September 21, 2023
Accepted: September 21, 2023
Published: October 12, 2023

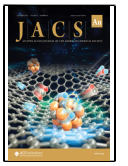

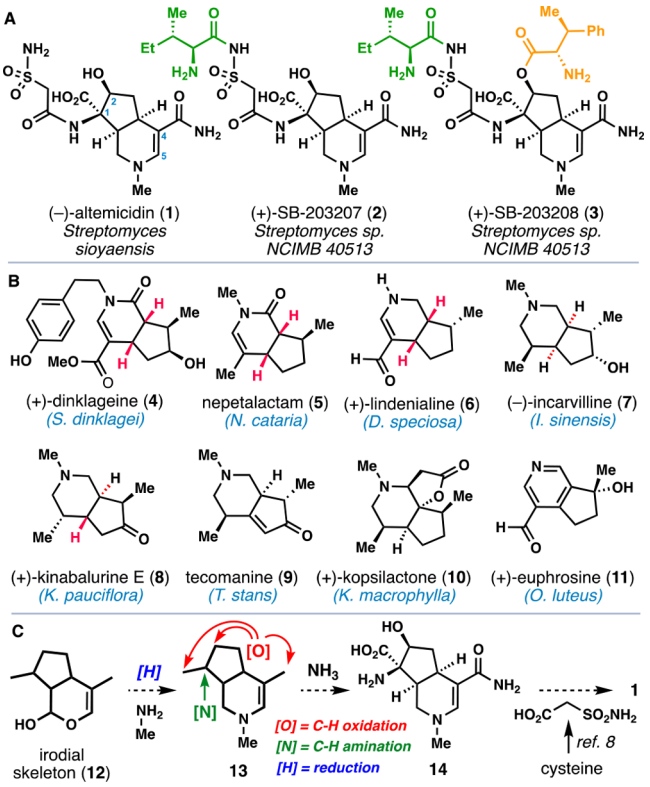

Figure 1. C10 alkaloids. (A) Altemicidin alkaloids from *Streptomyces sp.* (B) Plant-derived iridoid-type alkaloids. (C) Presumed biosynthesis of **1** during our synthetic studies.

Given this backdrop, a reasonable biosynthesis of **1** entailed conversion of the irodial skeleton **12** to **13** followed by multiple rounds of C–H oxidation, including a rare, tertiary C–H bond amination, to arrive at bicyclic amino acid **14** (Figure 1C).

Given their compact architectures, unusual array of polar functional groups, and intriguing medicinal value, synthetic interest in **1**–**3** has been steady over the last 4 decades.[10−15] Prior to our work, the groups of Kende and Kan reported routes to (−)-**1** and (+)-**2**, respectively, both in approximately 30 steps (Figure 2A). Kende's strategy leveraged the asymmetric Diels–Alder methodology of Reetz,[16] which uses chiral amino acid-derivatives as dienophiles. Kende and coworkers synthesized dienophile **15** from serine and found that it undergoes efficient cycloaddition with cyclopentadiene in the presence of diethylaluminum chloride to yield bicyclo[2.2.1]-heptene **16** in 87% yield. In this step, both the stereochemistry of the challenging quaternary *a,a*-amino stereocenter and the *cis*-ring fusion, which later becomes the 5,6-fused bicycle, are established. In five steps, **16** is converted into ketone **17** setting the stage for a Baeyer–Villiger oxidation of the norbornane skeleton, a feat that was accomplished using CF_3CO_3H. Following protecting group manipulations, lactone **18** was procured, and upon treatment with trifluoroacetic acid, it underwent deprotection and transannular cyclization to afford 5,6-fused azaindane bicycle **19** in quantitative yield. Despite this ingenious opening sequence, an additional 17 steps were required to convert **19** into (−)-**1**.

In 2014, building off prior work,[17] Kan reported a disparate strategy for the preparation of (+)-**2** featuring an intramolecular C–H insertion reaction (Figure 2A).[11] Chiral auxiliary bearing diazo ester **20** underwent allylic C–H insertion on the pendant cyclopentene ring catalyzed by $Rh_2(R\text{-DOSP})_4$. This pivotal transformation afforded 5,5-fused bicycle **21** with a 72% diastereomeric excess. This material

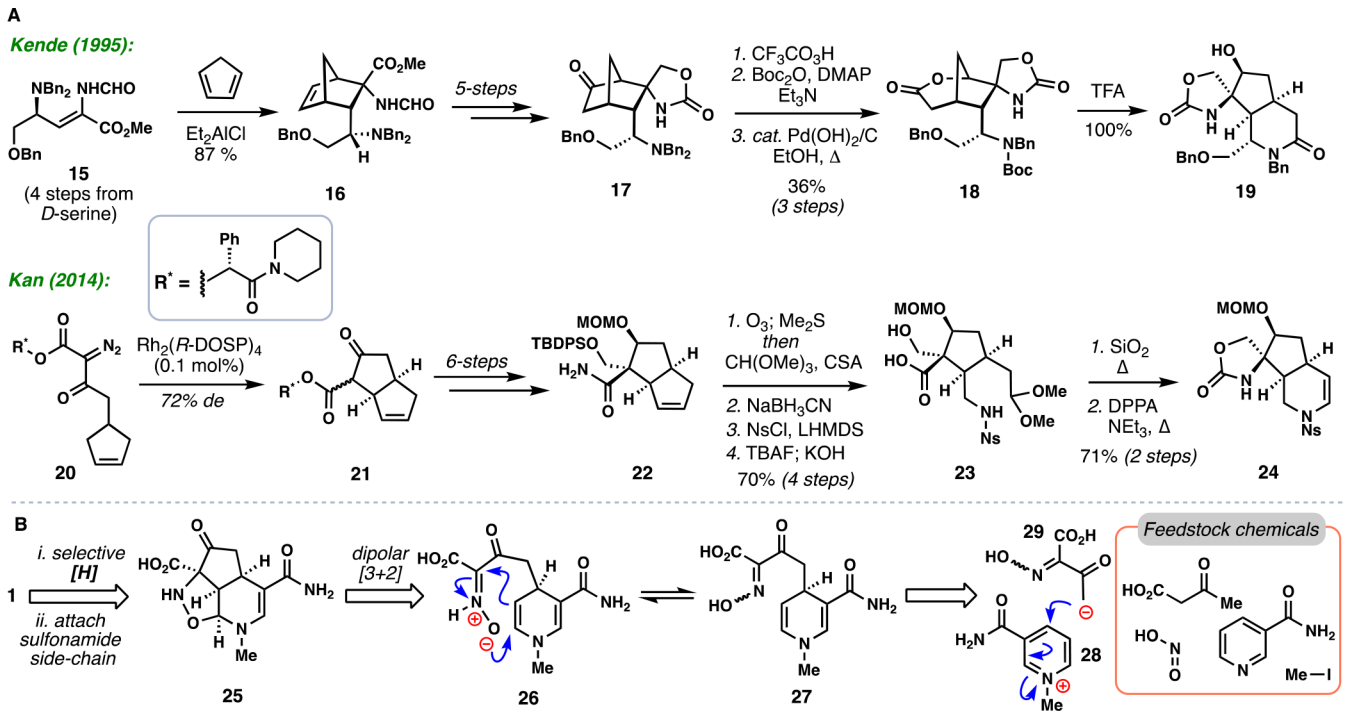

Figure 2. Strategies for the synthesis of altemicidin alkaloids. (A) Stepwise construction of the azaindane core in Kende's and Kan's routes to (−)-**1** and (+)-**2**, respectively. (B) Proposed dearomative annulation of nicotinamide for rapid entry into this alkaloid class. MOM = 2-methoxymethyl, Bn = benzyl, DMAP = 4-dimethylaminopyridine, and DPPA = diphenylphosphoryl azide.

https://doi.org/10.1021/jacsau.3c00417
JACS Au 2023, 3, 2883–2893

could be converted to amide **22** through a subsequent 6-step process. Ozonolytic cleavage of the cyclopentene ring (O_3, Me_2S, then camphorsulfonic acid (CSA) and $CH(OMe)_3$) revealed a mixed acetal/hemiaminal that could be reduced to the lactam by using sodium cyanoborohydride. Nosylation of lactam N−H followed by fluoride-induced desilylation and lactam hydrolysis gave acid **23**. These steps cleverly transferred the amide nitrogen of **22** to its correct position within the framework of **1**−**3**. To complete the synthesis of the altemicidin core, a silica-gel-mediated cyclization between the protected amine and acetal was used to generate the cyclic enamine moiety. A final Curtius rearrangement with DPPA revealed the hallmark quaternary amine stereocenter in the form of cyclic carbamate **24**. From **24**, an additional 15 steps were required to complete the synthesis of (+)-**2**.

While these past syntheses arrived at complex altemicidin cores with good stereocontrol, many synthetic manipulations and functional group interconversions were required to complete the final total syntheses. This observation weighed heavily in our own synthetic planning wherein we hoped that the use of native functional groups (or close derivatives) in the skeletal assembly process would limit the need for challenging functional group interconversions and protecting group manipulations on this dense and polar target molecule.[18] Given our research group's past successes in developing C−H activation-based routes to sesquiterpenes,[19−22] biomimetic strategies along the lines of Figure 1C were considered, but ultimately discarded as issues of chemoselectivity and protecting group manipulations/functional group interconversions would almost certainly arise.

Instead, we traced altemicidin back to tricyclic isoxazolidine **25** in the hopes that a single, chemoselective reduction of this compound, in combination with attachment of the sulfonamide side chain, could generate **1** directly (Figure 2B). Tricycle **25** can be viewed as the product of a formal [3 + 2] annulation, either via the depicted 1,3-dipolar cycloaddition (see **26**), or a polar stepwise process involving enamine addition to a polarized C−N π-bond and subsequent closure. Nitrone **26** appeared poised to arise from oxime **27** via prototropic tautomerization. Finally, oxime **27** could be taken back to simple, *N*-methylated nicotinamide salt **28** and a nucleophilic, four-carbon fragment (see **29**). Notably, the building blocks for this route are derived from the trivial feedstock chemicals acetoacetic acid and nicotinamide. Herein we describe a full account of our efforts to realize this strategy and the tactics that proved to be crucial along the way. This work is also placed into context with a recently described biosynthesis of **1** which parallels many of our synthetic ideas on how to rapidly construct this complex natural product and the challenges overcome by Nature.

RESULTS AND DISCUSSION

Dearomative Backbone Assembly

Our planned synthetic cascade was influenced by the rich history of dearomative pyridinium addition chemistry in the total synthesis of natural products.[23] In prior work by Kröhnke,[24] Comins,[25] Wenkert,[26] and Bosch,[27] pyridine activation by *N*-alkylation and nucleophilic enolate addition to the resulting pyridinium salt gave 1,6- and 1,4-dihydropyridines, often as highly unstable and unisolatable intermediates (Figure 3). To address the inherent instability of *N*-alkyl-1,4 dihydropyridines, the enamine was engaged in further bond-forming chemistry in situ, often via tautomerization to an iminium ion and subsequent trapping. Examples of this approach include the synthesis of vinoxine (**30**),[28] wherein the coupling of pyridinium salt **32** and enolate **33** is immediately followed by the protonation of the resulting dihydropyridine to induce a Pictet−Spengler cyclization and generate tetracycle **35** by way of iminium ion **34**. Similarly, the azabicyclo[4.3.1]nonane core of ervitsine (**31**)[29] was assembled by reacting the dihydropyridine formed from **36** and **37** with Eschenmoser's salt to form iminium ion **38** which cyclized to **39**. While these examples demonstrate that unstable dihydropyridines derived from enolate additions to *N*-alkylpyridines can be used in complexity-generating cascade processes, the yields of the aforementioned transformations are quite low.

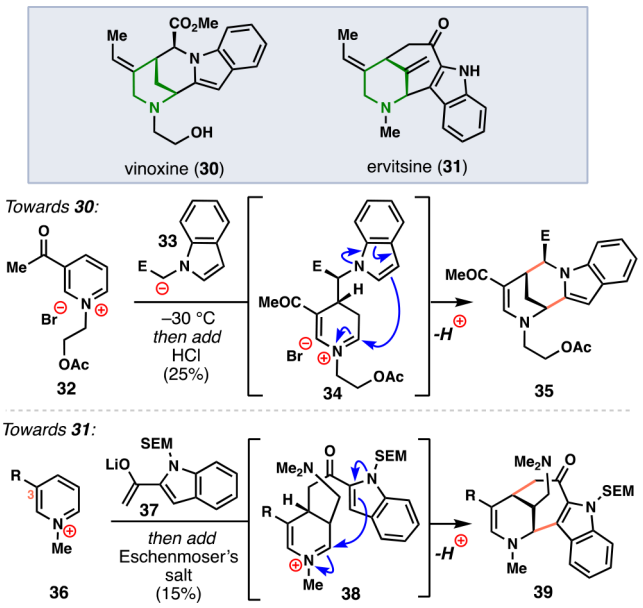

Figure 3. Examples of prior dearomative enolate addition cascades employing *N*-alkylpyridine salts in natural product synthesis. E = ester, SEM = 2-(trimethylsilyl)ethoxymethyl.

The impressive structural complexity of the bridged bicycles that emerge from the cascades shown in Figure 3 inspired our initial attempts toward **1** (Figure 4A). We questioned whether an α-ketoxime nucleophile (see **40**) might serve the dual purpose of a nucleophile, via the ketone enolate, and subsequent electrophile, via the oxime C−N π-bond, and enable a cascade acting as a formal equivalent to a concerted dipolar cycloaddition (see **42** → **43** → **44**). We prepared the nicotinonitrile-derived *N*-methylpyridinium salt **41** and explored its reactivity with various nucleophiles. Using the free oxime (**40**, R = H), the formation of tricycle **44** was never detected under a variety of basic conditions, including lithium enolate generating conditions; instead, complex mixtures and extensive decomposition were typically observed. When employing the *O*-benzyl oxime (**40**, R = Bn) we detected trace amounts (~5%) of conjugated, oxidized adduct **45**, consistent with many prior observations on the reactivity and instability of *N*-alkyl, 1,4-dihydropyridines.[30] Thoroughly excluding oxygen did not abate the formation of **45**, and the addition of oxidants, such as sodium persulfate or DDQ also did not promote its formation in higher yields. Exploring alternatives to this challenging, direct addition reaction, we found that silyl enol ether **46** could be cross coupled with 4-

https://doi.org/10.1021/jacsau.3c00417
JACS Au 2023, 3, 2883−2893

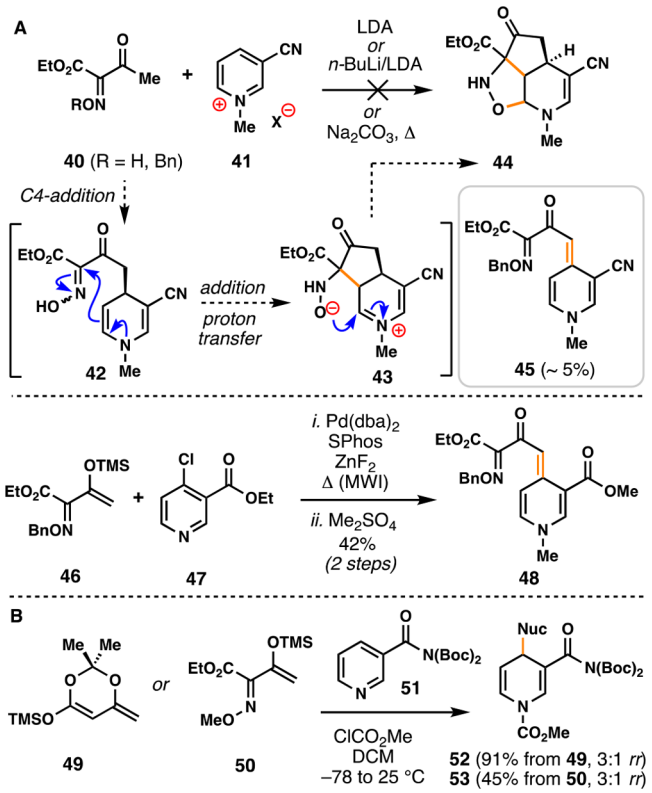

Figure 4. Initial pyridine dearomatization studies. (A) Attempts to forge the azaindane core in a single step. X = I or OTf. (B) Successful pyridinium addition employing chloroformate activation. MWI = microwave irradiation.

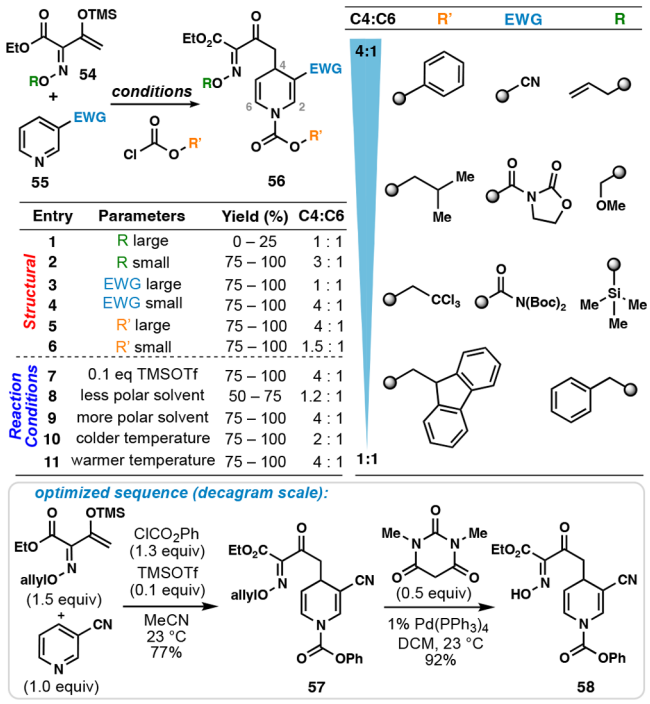

Figure 5. Optimization studies of the pyridinium addition reaction and the scalable synthesis of adduct **58**.

chloro-ethylnicotinate (**47**) resulting in dienamine **48** after pyridine *N*-methylation with dimethyl sulfate. While this procedure offered an improved yield (42% over two steps), we were unable to reduce the α,β-unsaturated ketone moiety, hampering efforts to advance this compound.

Turning toward *N*-acylpyridinium chemistry, which can deliver stable dihydropyridine adducts,[31] we reacted *N,N*-bisBoc-nicotinamide (**51**) with several nucleophilic fragments using standard methyl chloroformate activation (Figure 4B). Gratifyingly, both silyl ketene acetal **49** and silyl enol ether **50** reacted to give addition products **52** or **53** in 91% and 45% yield, respectively, and with ~3:1 selectivity favoring the 1,4-addition product in both cases. Notably, the lithium, sodium, or titanium enolates of **40** were not competent coupling partners in this process.[32,33] Given the high yield of adduct **52**, we evaluated its suitability toward advancement to the azaindane core of altemicidin; however, our efforts to introduce imine or oxime functionality onto the β-keto ester were unsuccessful.[34] Given these challenges, efforts were undertaken to improve the coupling yield of **50** or of related derivatives (Figure 5).

The key challenges encountered during the addition of α-keto-oxime silyl enol ethers to *N*-acylpyridinium salts included sluggish conversion and reaction stalling (30% conversion at 12−18 h), instability of the dihydropyridine product to typical aqueous workup, and variable or minimal C4/C6 regioselectivity (~1.1:1) in some cases. To avoid *in situ* deprotection of the silyl enol ether and stalled reactions, we initially added it portionwise over 36 h (4−6 equiv added). Analysis of aliquots of the reaction mixture by ^{1}H NMR spectroscopy showed that this boosted conversion from 30 to 70%; however, isolated yields of product after workup of the bulk reaction mixture remained low (typically ~40%). We determined that the coupled product could revert to starting material depending on workup conditions employed, but dropwise, reverse addition of the cooled reaction mixture to aqueous NaOH (1 M) resolved this issue. We subsequently examined the influence of the oxime nucleophile (**54**), electron-withdrawing group at the pyridine C-3 position (**55**), and chloroformate activator on product formation and positional selectivity (Figure 5 table).[35,36] Generally, larger protecting groups on the oxime oxygen, such as trimethylsilyl or benzyl, resulted in diminished product formation and selectivity relative to allyl or methoxymethyl moieties (entries 1 and 2). In accordance with well-appreciated effects in *N*-acylpyridinium chemistry,[23] C-4 regioselectivity was diminished by increasing the steric bulk of the electron-withdrawing group at the pyridine C-3 position, with a cyano group outperforming various carbamates (entries 3 and 4). Additionally, phenyl chloroformate proved to be the best activator for promoting C-4 addition and was superior to isopentyl, trichloroethyl, and Fmoc-based chloroformates (entries 5 and 6).

While these studies identified *O*-allyl silyl enol ether with phenyl chloroformate-activated-nicotinonitrile as the optimal pairing, numerous equivalents (up to 4−5) of nucleophile were required to reach reaction completion, a problem we suspected could be related to an unfavorable pyridine ⇌ pyridinium equilibrium in our system and its competition with simple silyl deprotection. When TMSOTf was added to the reaction mixture,[37,38] only 1.5 equiv of the silyl enol ether was required to achieve full conversion of nicotinonitrile within 30 min, and the overall yields of the combined C-4 and C-6 dihydropyridine adducts exceeded 90% (compared to 70% without additive). In less polar solvents, the reaction was sluggish and we observed precipitation of the pyridinium salt out of solution. Of note, regioselectivity for the C-4 adduct was only

https://doi.org/10.1021/jacsau.3c00417
JACS Au 2023, 3, 2883−2893

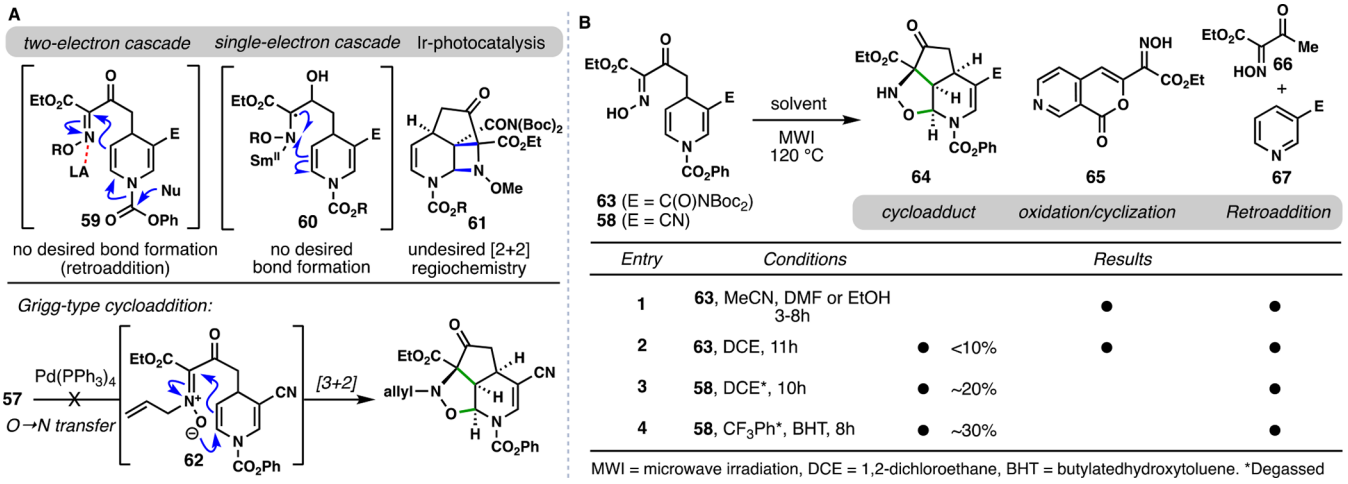

Figure 6. Initial forays into the formation of the azaindane core of altemicidin. (A) Unsuccessful attempts to manipulate the dihydropyridine nucleus. (B) Thermal cycloaddition studies.

preserved using substoichiometric quantities of TMSOTf (0.1 equiv); when stoichiometric TMSOTf was employed, the reaction was nearly instantaneous, but regioselectivity was completely eroded. Cooling the reaction to 0 °C negatively impacted regioselectivity, and warming the reaction to 50 °C did not improve it. We also observed that increasing the steric bulk of the silyl triflate to TIPS or TBSOTf decreased regioselectivity. This stands in contrast to the typical positive correlation between chloroformate steric bulk and C-4 regioselectivity and supports *N*-chloroformate activation of the pyridine rather than an alternative *N*-silylium activation pathway.[39] With these findings in hand, a robust route to **57** (77% isolated yield) became possible, and following mild cleavage of the allyl protecting group (1 mol % $Pd(PPh_3)_4$, 0.5 equiv of NDMBA), a decagram-scale route to free oxime **58** was achieved (Figure 5).

Cyclization Studies

We next investigated multiple strategies to form the altemicidin cyclopentane ring, thus completing the full azaindane core and the key α-tertiary amino stereocenter (Figure 6A). Efforts to simultaneously cleave the phenyl carbamate and engage the resulting free enamine in an addition reaction to the oxime C−N π−bond (see **59**) failed owing to retro-addition of the ketone nucleophile and decomposition. Isolation of the free dihydropyridine could also not be achieved in a preparative manner. Radical-based conditions were also considered for this challenging step, wherein a single-electron reduction of the oxime π−bond and radical cyclization onto the enamine C−C π-bond would lead to ring formation (see **60**). Unfortunately, treating various oxime starting materials with samarium diiodide did not promote this coupling. Inspired by recent work from Schindler and co-workers on azetidine formation by alkene/oxime [2 + 2] photo cycloadditions, we subjected our oxime to blue light irradiation in the presence of $[Ir(dF(CF_3)ppy)_2(dtbbpy)](PF_6)$,[40] but found that coupling occurred at the electron-deficient alkene, thus forming congested azetidine **61**. Our previous success at removing the allyl protecting group (see **57** → **58**, Figure 5) prompted us to consider Grigg's palladium-mediated oxime *O* → *N*−allyl migration for the in situ generation of nitrones and (see **62**) their subsequent participation in dipolar cycloadditions (Figure 6A).[41] Subjecting **57** to these conditions ($Pd(PPh_3)_4$, Δ), however, only led to partial deallylation or decomposition at elevated temperatures.

Given these failures, we undertook cyclization studies of oximes **63** and **58** under purely thermal conditions hoping to leverage oxime-nitrone tautomerization in a subsequent dipolar cycloaddition (Figure 6B). Conventional heating of **63** in a variety of solvents gave minimal formation of **64** (<5%). Microwave heating of **63** in polar solvents (MeCN, DMF, EtOH) did not produce any productive cycloadducts, but rather gave aromatized product **65**, along with significant retro pyridinium addition products (entry 1). In dichloroethane (DCE), however, microwave irradiation of **63** at 120 °C gave desired altemicidin tricycle **64** in 10% yield, albeit with formation of **65** and **67** (entry 2).[42] Under degassed conditions, oxime **58** proved to be a superior substrate, forming **64** in a 20% yield (entry 3). Using trifluorotoluene as a solvent and including BHT as a radical scavenger increased the yield of **64** to 30% (entry 4). Despite these improvements, retro pyridinium addition remained a significant cause of lost material, and our challenges were further compounded by the instability of tricyclic ketone **64** on silica gel. In our initial synthetic planning, we wanted to leverage the concavity of **64** (or **25**, Figure 1) to elicit a stereoselective reduction of the ketone and produce the altemicidin secondary alcohol with the correct stereochemistry. However, in our hands, reducing **64** proved problematic, as only complex mixtures were formed with hydride reducing agents.

Given these challenges, we reasoned that ketone reduction prior to cycloaddition might avoid retro-addition and impart greater conformational flexibility for a more efficient cycloaddition (Figure 7). We reduced ketone **58** ($NaBH_4$, 2% MeOH/THF, − 50 °C) to secondary alcohol **68** in 65% yield as a combined mixture of diastereomers (*dr* = 1.7:1) and subjected this mixture to the previously established microwave conditions in trifluorotoluene. Gratifyingly, this produced tricycle **69** in 80% combined yield, over double the yield seen for substrate **63**/**58**. The alcohol epimers of **69** could also be efficiently separated by column chromatography to yield the desired diastereomer in 50% overall yield. Moreover, we could further telescope this reaction through the phenyl carbamate removal by the addition of a methanolic solution of LiBr−DBU to the cooled cycloaddition reaction mixture thus generating free amine **70** in 45% isolated yield (Figure

https://doi.org/10.1021/jacsau.3c00417
JACS Au 2023, 3, 2883−2893

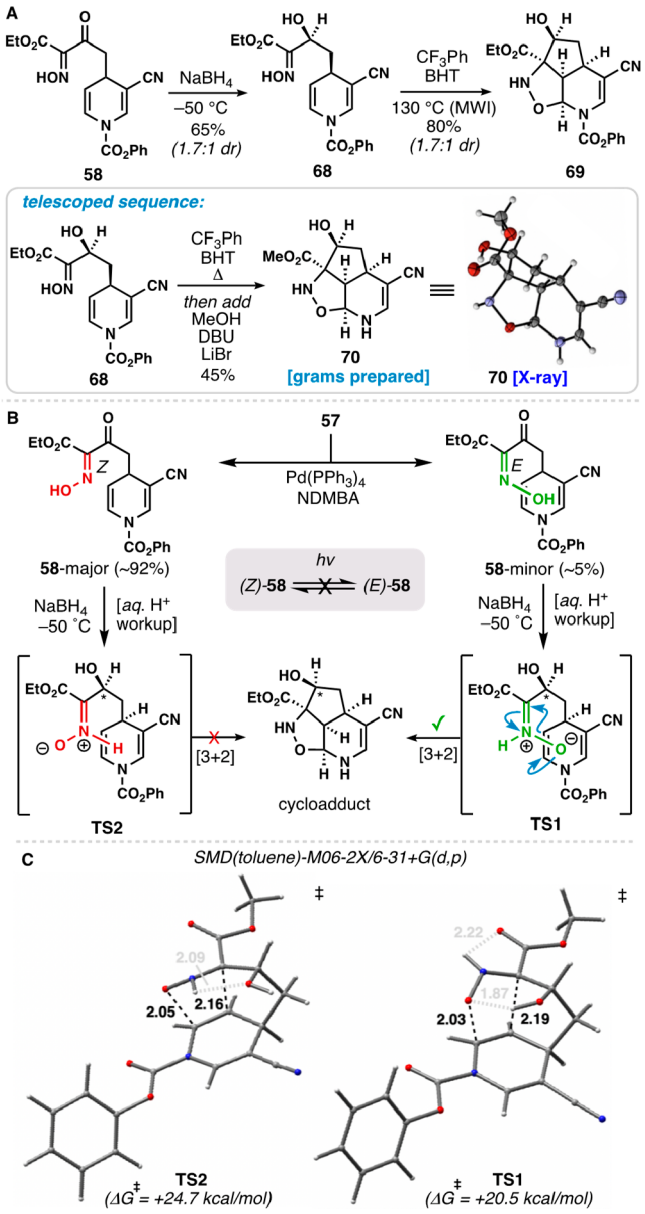

Figure 7. Development of a preparative route to the altemicidin core. (A) Efficient nitrone/alkene dipolar cycloaddition. (B) Insight into the cycloaddition process. (C) Dipolar cycloaddition transition state structures as determined by DFT.

7A).[43,44] We have produced over 5 g of **70** using this procedure.

On scaling up batches of **58**, we found that the palladium-mediated deallylation of **57** gave a mixture of oxime isomers that could be separated by column chromatography (Figure 7B). A major isomer (**58**-major), which accounted for most of the material (92% yield), was isolated along with a 5% yield of a minor geometric isomer (**58**-minor). We then subjected these compounds independently to the $NaBH_4$ reduction. **58**-major gave the expected secondary alcohol intermediate as a mixture of alcohol epimers, while the minor isomer of **58** produced quantities of the tricyclic ring system directly. Analysis of this reaction by TLC showed conversion of **58**-minor to the corresponding alcohol at −50 °C, followed by cyclization and concomitant carbamate removal upon acidic workup to generate the full tricyclic cycloadduct under mild conditions. Because of the apparent lower reaction barrier for the cyclization of **58**-minor, we believe that this isomer possesses the *E*-oxime configuration which is predisposed to dipolar cycloaddition following tautomerization to a reactive nitrone (see **TS1**, Figure 7). Density functional theory (DFT) calculations at the SMD(toluene)-M06-2*X*/6-31+G(d,p) level of theory (see the Supporting Information) also indicated a lower activation barrier for this dipolar cycloaddition relative to its nitrone isomer with a difference in free energy barriers of 4.2 kcal mol^{-1} (see **TS1** vs **TS2**, Figure 7C).[45,46] In both calculated structures, the secondary hydroxyl group engages in hydrogen bonding with the nitrone. The forcing conditions needed in our thermal, microwave-mediated cyclization ($PhCF_3$, 130 °C) may therefore be related to the oxime → nitrone isomerization/tautomerization process. We also note that samples of **58**-minor convert to **58**-major over time even when stored cold, thus indicating a thermodynamic preference for the *Z*-configured oxime. While UV irradiation is known to promote oxime isomerization reactions,[47] this maneuver primarily led to decomposition in our system.

Chemoselective Core Manipulation

With a tricyclic core structure rapidly constructed, we viewed removal of the extraneous oxygen atom from the isoxazolidine ring as the principal remaining task toward altemicidin (Figure 8). This proved challenging and required significant reagent evaluation across multiple substrates. Cycloadduct **70** could be bis-acetylated to yield **71**, which then allowed us to cleanly methylate the free nitrogen (NaH, MeI) in high yield generating isoxazolidine **72** (Figure 8A). With **70**-**72** in hand, we proceeded to evaluate their reactivity with reducing agents common to N−O bond reduction (Figure 8B). Samarium diiodide in methanol cleanly gave N−O bond reduction product **77** (entry 1), but when water was added as a cosolvent,[48] the more powerful reducing agent extensively reduced the cyclopentane ring (entry 2). Standard hydrogenolysis conditions (entry 3) completely reduced the amino acrylonitrile to a methylpiperidine but left the N−O bond untouched (entry 3). Surprisingly, Zn^0/AcOH was completely ineffectual toward any reduction (entry 4). Success was eventually realized by moving toward molybdenum(0) reagents, which are known to perform deoxygenation and N−O bond reduction reactions.[49,50] When tricycle **71** was reacted with one equivalent of $Mo(CO)_6$ in wet, refluxing acetonitrile, dihydropyridine **76** was formed as the sole reaction product (entry 5). Formation of this dihydropyridine signified that the desired N−O reduction had occurred along with elimination to form an intermediate iminium, which had undergone tautomerization. Excited by the possibility that this iminium might be intercepted by a suitable hydride donor to deliver the desired reduced core, we searched for exogenous hydride donors that could be compatible with $Mo(CO)_6$.

We initially introduced excess phenylsilane to our reaction mixture (entries 6−9).[51] In the case of substrate **71**, this gave desired product **75** in 4-fold excess over the undesired dihydropyridine **76** and in 40% overall yield (entry 7). Notably the electron-withdrawing acetate group on nitrogen is crucial for this process, as substrate **70** decomposed under these conditions (entry 6). Increasing the phenylsilane equivalents from four to ten proved beneficial, generating a near 20:1 mixture of **75**:**76** in 60% overall yield. When carrying out this double reduction on *N*-methylated compound **72** (entry 9), however, we observed only a N−O bond reduction.

https://doi.org/10.1021/jacsau.3c00417
JACS Au 2023, 3, 2883−2893

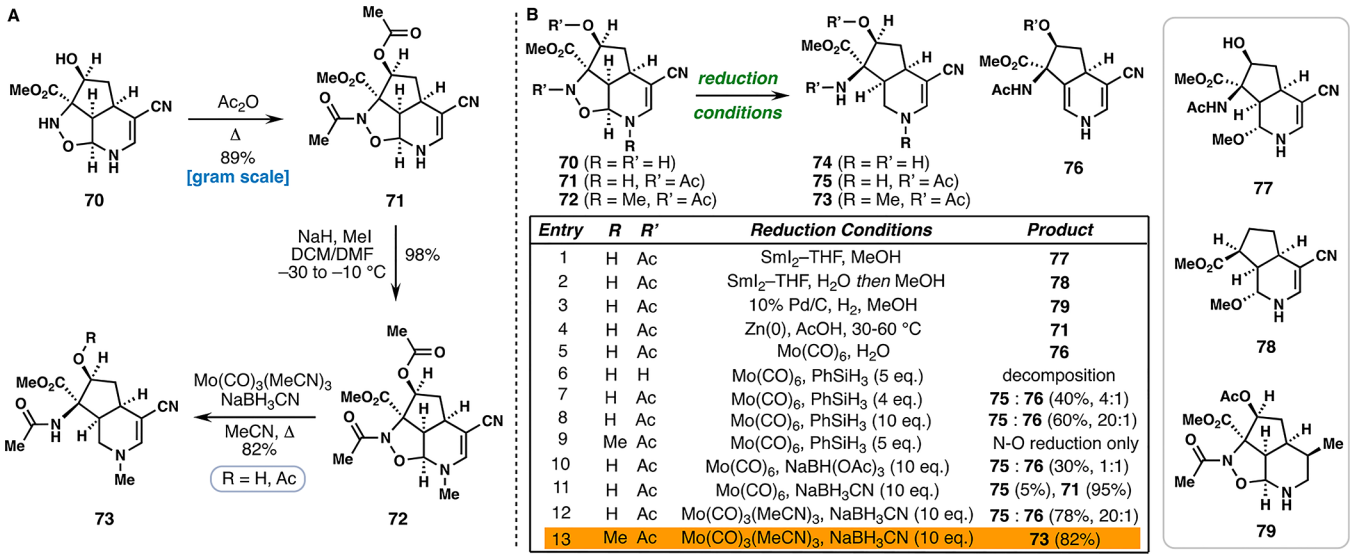

Entry	R	R'	Reduction Conditions	Product
1	H	Ac	SmI_2–THF, MeOH	**77**
2	H	Ac	SmI_2–THF, H_2O *then* MeOH	**78**
3	H	Ac	10% Pd/C, H_2, MeOH	**79**
4	H	Ac	Zn(0), AcOH, 30-60 °C	**71**
5	H	Ac	$Mo(CO)_6$, H_2O	**76**
6	H	H	$Mo(CO)_6$, $PhSiH_3$ (5 eq.)	decomposition
7	H	Ac	$Mo(CO)_6$, $PhSiH_3$ (4 eq.)	**75** : **76** (40%, 4:1)
8	H	Ac	$Mo(CO)_6$, $PhSiH_3$ (10 eq.)	**75** : **76** (60%, 20:1)
9	Me	Ac	$Mo(CO)_6$, $PhSiH_3$ (5 eq.)	N-O reduction only
10	H	Ac	$Mo(CO)_6$, $NaBH(OAc)_3$ (10 eq.)	**75** : **76** (30%, 1:1)
11	H	Ac	$Mo(CO)_6$, $NaBH_3CN$ (10 eq.)	**75** (5%), **71** (95%)
12	H	Ac	$Mo(CO)_3(MeCN)_3$, $NaBH_3CN$ (10 eq.)	**75** : **76** (78%, 20:1)
13	Me	Ac	$Mo(CO)_3(MeCN)_3$, $NaBH_3CN$ (10 eq.)	**73** (82%)

Figure 8. Studies on chemoselective isoxazolidine reduction. (A) Successful synthesis of the altemicidin core. (B) Selected reduction optimization studies.

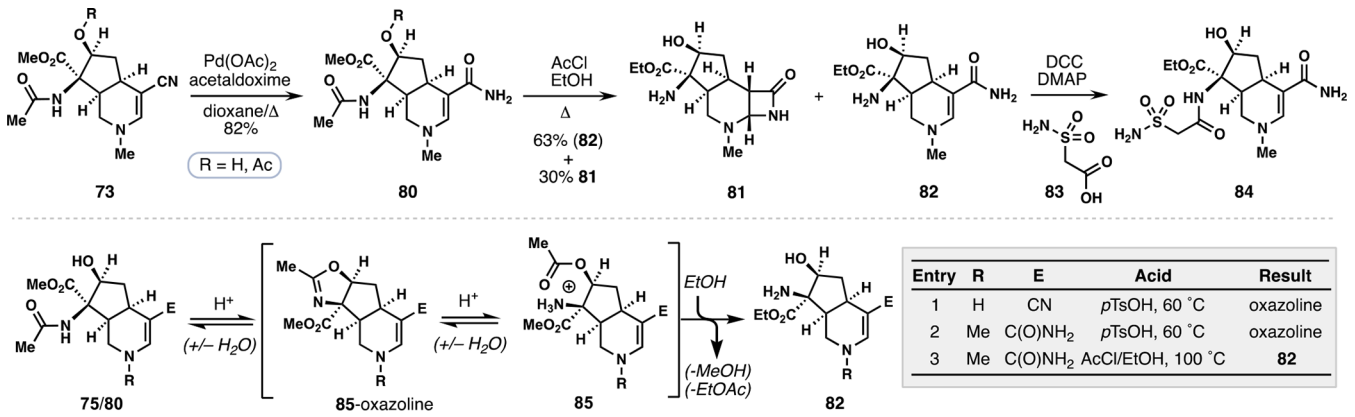

Entry	R	E	Acid	Result
1	H	CN	*p*TsOH, 60 °C	oxazoline
2	Me	$C(O)NH_2$	*p*TsOH, 60 °C	oxazoline
3	Me	$C(O)NH_2$	AcCl/EtOH, 100 °C	**82**

Figure 9. Synthesis of advanced sulfonamide **84** required a challenging acetamide cleavage.

Other external hydride sources, including sodium triacetoxy borohydride (entry 10) and sodium cyanoborohydride (entry 11) were evaluated in concert with $Mo(CO)_6$, but these reducing systems showed poorer reactivity. With substrate **71**, $NaBH(OAc)_3$ generated an equimolar amount of desired product **75** and dihydropyridine **76** (30% combined yield). While **75** was the sole product formed with $NaBH_3CN$, the conversion was very poor. A report detailing the reaction of sodium cyanoborohydride with $Mo(CO)_6$ suggested to us that perhaps undesired cross-reactivity occurred, and that distinct (and unproductive) reducing species might be generated under these conditions.[52] Since $Mo(CO)_3$ $(MeCN)_3$ is presumably generated in situ from $Mo(CO)_6$ under our reaction conditions, we preformed $Mo(CO)_3$ $(MeCN)_3$ by heating $Mo(CO)_6$ at reflux for several hours in acetonitrile, and then added tricycle **71** to the mixture along with excess $NaBH_3CN$ (entry 12). Pleasingly, we obtained a 20:1 mixture of **75**:**76** in 78% combined yield. Most importantly, subjecting *N*-methylated substrate **72** to these conditions generated reduced product **73** exclusively in 82% isolated yield (entry 13).

Since only the *N*-acetamide activating group was compatible with our optimized molybdenum-based reduction conditions, we investigated removal of this moiety in preparation for sulfonamide side-chain attachment (Figure 9). Again, this transformation proved to be challenging and needed to be evaluated on multiple substrates. Mild nitrile hydrolysis ($Pd(OAc)_2$, acetaldoxime, Δ) smoothly converted **73** to amide **80**, again as a mixture of inconsequential mono and bis-acetylated products. The acetamide group proved resilient to base-mediated cleavage, and surprisingly many conditions also did not hydrolyze the ester—foreshadowing future challenges (*vide infra*). Charette's selective amide reduction sequence and variations thereof gave complex mixtures.[53] While mild acids, such as acetic acid, only returned starting material, heating **73** or **75** with *p*-toluenesulfonic acid (*p*TsOH) at 60 °C forged an oxazoline ring, possibly offering us a way forward via an N → O acyl transfer mechanism (see **85**) and ester cleavage pathway.

To this end, a large panel of acids, solvents, and reaction temperatures were explored with very few positive outcomes. In many cases, the reaction stalled at the oxazoline stage or produced the desired product only in minor quantities as part of a highly complex mixture. Complete cleavage of the acetyl group occurred only under the mediation of rigorously water-free 10 M HCl (formed in situ by reacting acetyl chloride with ethanol) at 100 °C, conditions that also promote trans-esterification of the methyl ester to an ethyl ester. Under these conditions, substrate **80** was converted to **82** in 63% isolated

https://doi.org/10.1021/jacsau.3c00417
JACS Au 2023, 3, 2883–2893

yield.[54] In addition, β-lactam **81** (31%) was also formed in analogy to observations by Uriac on a related vinylogous amide.[55] Despite the strained nature of **81**, we were unable to isomerize it to **82**. Efforts to minimize the formation of **81** were unsuccessful, and even minor deviations from the EtOH/AcCl protocol tended to engender the formation of complex mixtures, some of which showed increased β-lactam formation. Notably both *N*-acetamide **73** or its purified oxazoline form could be subjected to these conditions, and both yielded the corresponding products in similar yields and ratios, indicating that an oxazoline is a viable intermediate along this reaction pathway. Finally, amide **82** could then be coupled with sulfonamide-containing acid **83** (DCC, DMAP) to yield ethyl altemicidin (**84**) in 73% yield thus setting the stage for a final ester hydrolysis to altemicidin.[56]

Much to our dismay, subjecting **84** to typical ester hydrolysis conditions, ranging from mild (e.g., Me_3SnOH) to forcing (e.g., KOH, reflux), was ineffective (Figure 10). We had

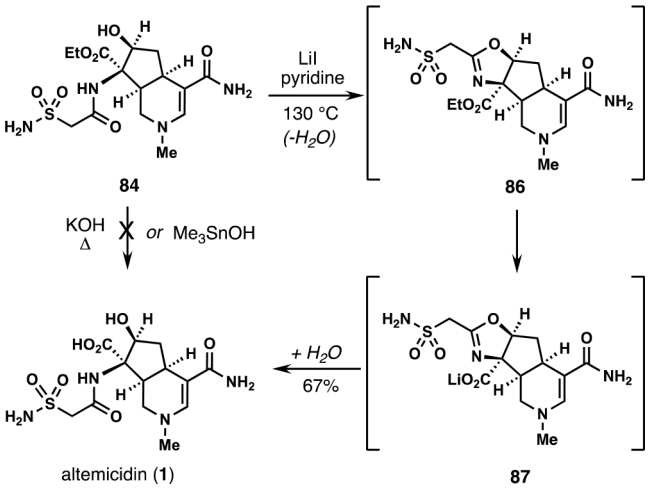

Figure 10. A complex dealkylation pathway enables the completion of the total synthesis of altemicidin.

anticipated challenges at this stage of the synthesis as we noted that Kende and Fukuyama's prior syntheses required somewhat unorthodox maneuvers to accomplish this task, namely, demethylation of a methyl ester using lithium *n*-propyl mercaptide in HMPA or hydrogenation of a diphenylmethyl (Dpm) ester, respectively. Moreover, in both past syntheses, these transformations were performed on advanced intermediates that bore the sulfonamide side chain.

We had previously observed facile ester hydrolysis of tricycles **70**, **85**-oxazoline, and acetamide hydrolysis product **82** during our synthetic studies. In fact, we even had to buffer our aqueous workup solutions in certain instances to prevent unwanted saponification. In contrast, acetamide **80**, like ethyl altemicidin (**84**), was not sensitive to base. We attributed this pattern of reactivity to steric congestion about the amine stereocenter due to the acetamide or sulfonamide side chain. In both tricycles **70** and **85**-oxazoline, the amine is constrained within a ring, and **82** lacks the acetamide entirely; as a result, these intermediates undergo saponification readily. In contrast, acylation at the amine in **80** and **84** prevents access to the ester (or disfavors formation of a tetrahedral intermediate), thus rendering hydrolysis difficult.

We briefly attempted to leverage the ease of saponifying **82**, by inverting the order of operations for our endgame sequence. Hydrolysis of **82** using KOH/H_2O generated the carboxylic acid, but we were unable to convert this intermediate to the natural product. Guided by the precedents of Fukuyama and Kende, we explored the synthesis of a benzyl ester intermediate as well as ester dealkylation processes to reach the carboxylic acid. Toward the former effort, a benzyl ester of **80** could be synthesized but did not survive the harshly acidic ethanol conditions used for acetamide cleavage. As a result, we still obtained product **82**. In our survey of dealkylation conditions, we found that lithium iodide in refluxing pyridine mediated conversion of the ethyl ester to the corresponding acid (Figure 10). To our initial great disappointment, however, we found that LiI/pyridine-mediated conditions did not generate altemicidin but instead oxazoline, **87**. As we repeated this reaction, we detected that small (<5%), but inconsistent quantities of altemicidin (**1**) were formed; however, no further modification of the reaction conditions themselves gave us the natural product directly. Instead, we noticed that oxazoline **87**, when left in D_2O in an NMR tube on the benchtop, rehydrated slowly to altemicidin over several days. Ultimately, we found that our aqueous HPLC fractions could be heated to 30 °C for several hours before being concentrated to yield pure altemicidin in a 67% yield from **84**. Again, we find it likely that fortuitous oxazoline formation renders the ester more reactive toward dealkylation as steric hindrance is reduced.

A Surprise Ending

Following the completion and publication of our total synthesis of **1**, Abe and co-workers reported their findings on the biosynthesis of **1** (Figure 11).[57] As noted earlier, these researchers had previously identified the enzymatic origin of the sulfonamide side-chain as being cysteine-derived,[8] but studies on the azaindane core had not been disclosed, and most literature suggested that this fragment was derived through a monoterpene biosynthetic pathway as discussed previously.

The discovery of the *Streptomyces sp. sbz* gene cluster governing the enzymatic production of altemicidin proved quite surprising from both chemical and enzymatic standpoints (Figure 11). First, the biosynthetic building blocks of the azaindane core of **1** were identified as *S*-adenosyl methionine (SAM) and β-Nicotinamide adenine dinucleotide (β-NAD) thus revealing a nonterpenoid origin of this alkaloid. While β-NAD is commonly found in primary metabolism, this work signifies its first appearance as a secondary metabolite building block.[58] Also of note, the entire amino acid side chain of SAM is incorporated into **1**, highlighting its utility as more than a methyl group donor in this context.[59]

SAM and β-NAD are merged by the pyridoxal phosphate (PLP)-dependent enzyme SbzP which carries out a biosynthetically unprecedented annulation cascade reaction (Figure 11).[60] Abe and co-workers propose that upon condensation of SAM and PLP, AdoSMe is eliminated, generating extended enamine **88**. In the active site of SbzP, this nucleophilic species engages β-NAD in a pyridinum addition reaction leading to dihydropyridine **89**. Utilizing lysine side-chain residue K334, species **90**, which contains an electrophilic C═N π-bond, is generated and reacted with the neighboring enamine leading to annulated intermediate **91**. Following tautomerization and cofactor release, dihydropyridine **92** is generated. The oxidative enzyme SbzQ then carries out hydroxylation of the cyclopentane ring, generating **93**.

https://doi.org/10.1021/jacsau.3c00417
JACS Au 2023, 3, 2883−2893

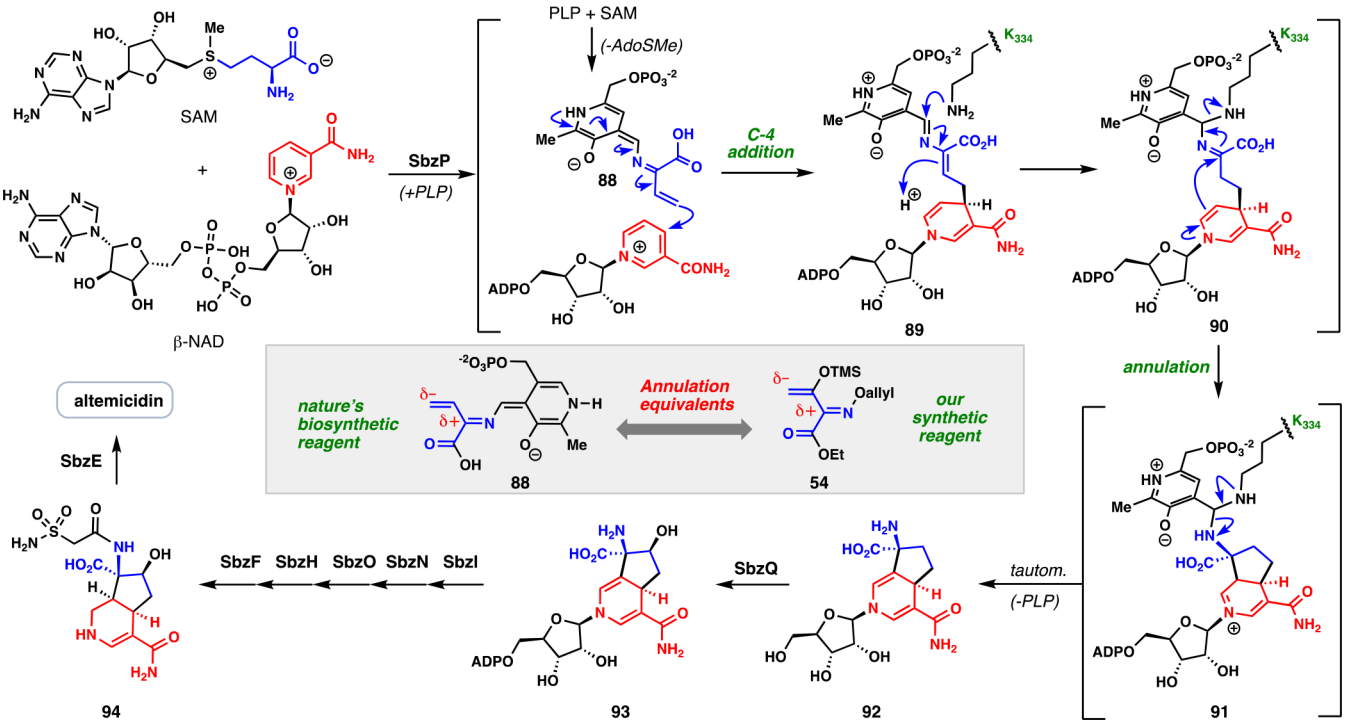

Figure 11. Abe's biosynthetic studies of altemicidin reveal an unexpected and unprecedented dearomative pyridinium addition/annulation cascade to generate the azaindane core of the natural product.[57] Cofactor generated intermediate **88** mirrors the polarity of synthetic annulation reagent **54**. Figure adapted with permission from ref 57. Copyright 2021 Springer.

Finally, downstream biosynthetic enzymes carry out a suite of tailoring reactions to process **93** into **1**.

Nature's synthetic blueprint and our initial cascade attempts toward **1** are eerily similar in that they utilize nicotinamide salts and 4-carbon annulation fragments of similar polarity (compare **88** and **54**). SbzP, however, can shield sensitive intermediates such as **89** and **90** from deleterious oxidation processes, thus allowing the second step of the cascade to ensue—a process we failed to control in the laboratory. While C–C bond-forming pyridinium addition reactions have remained a mainstay in synthetic heterocyclic chemistry for decades, they now appear in the biosynthetic lexicon as well.

CONCLUSION

In this article, we have chronicled the development of a total synthetic strategy toward the compact and polar alkaloid altemicidin.[61] Our dearomative strategy introduced all skeletal complexity quickly, and significant experimentation and reconnaissance gathering was needed to successfully maneuver functional group interconversion in this polar, heteroatom-laden landscape. Key to these efforts was the discovery of the Mo^0/$NaCNBH_3CN$-mediated reduction, which essentially "erased" the dipolar cycloaddition oxygen atom in a chemoselective fashion. Several unanticipated oxazoline intermediates were also productively leveraged to facilitate challenging transformations. In total, a greatly reduced step count was the reward for these investments as only 13 steps were needed to reach the natural product—fewer than half the steps of past routes. Biomimetic logic often profoundly shapes synthetic planning, and has even allowed for the predictions of new, yet-to-be isolated secondary metabolites.[62] Our work on **1** represents a rare case where a strictly abiotic synthetic strategy turned out to strongly parallel the enzymatic pathway used in nature. We can only assume other similar surprises await those investigating the chemistry and biology of complex natural products.

ASSOCIATED CONTENT

Supporting Information

The Supporting Information is available free of charge at https://pubs.acs.org/doi/10.1021/jacsau.3c00417.

Experimental procedures and spectroscopic data (PDF)

AUTHOR INFORMATION

Corresponding Author

Thomas J. Maimone − *Department of Chemistry, University of California, Berkeley, Berkeley, California 94720, United States;* orcid.org/0000-0001-5823-692X; Email: maimone@berkeley.edu

Authors

Claire S. Harmange Magnani − *Department of Chemistry, University of California, Berkeley, Berkeley, California 94720, United States;* orcid.org/0000-0003-0334-2535

José R. Hernández-Meléndez − *Department of Chemistry, University of California, Berkeley, Berkeley, California 94720, United States*

Dean J. Tantillo − *Department of Chemistry, University of California−Davis, Davis, California 95616, United States;* orcid.org/0000-0002-2992-8844

Complete contact information is available at: https://pubs.acs.org/10.1021/jacsau.3c00417

Notes

The authors declare no competing financial interest.

https://doi.org/10.1021/jacsau.3c00417
JACS Au 2023, 3, 2883−2893

■ ACKNOWLEDGMENTS

Financial support is acknowledged from the NIH NIGMS (R01GM136945 to T.J.M). C.S.H.M. acknowledges the National Science Foundation for a Graduate Research Fellowship. J.H.M. is appreciative to the Berkeley Amgen Scholars Program for supporting a summer research internship. We thank Katerina Gorou for helpful discussions and Prof. Ikuro Abe (University of Tokyo) for providing an authentic sample of altemicidin. We are grateful to Dr. Hasan Celik and Dr. Jeffrey Pelton for NMR spectroscopic assistance and NIH grants GM68933 and S10OD024998. Dr. Nicholas Settineri is acknowledged for X-ray crystallographic analysis wherein support from NIH Shared Instrument Grant (S10-RR027172) is also acknowledged.

■ REFERENCES

(1) Takahashi, A.; Kurasawa, S.; Ikeda, D.; Okami, Y.; Takeuchi, T. Altemicidin, A New Acaricidal and Antitumor Substance I.Taxonomy, Fermentation, Isolation and Physico-Chemical and Biological Properties. *J. Antibiot. (Tokyo)* **1989**, *42*, 1556.

(2) Takahashi, A.; Ikeda, D.; Nakamura, H.; Naganawa, H.; Kurasawa, S.; Okami, Y.; Takeuchi, T.; Iitaka, Y. Altemicidin, A New Acaricidal and Antitumor Substance II. Structural Determination. *J. Antibiot. (Tokyo)* **1989**, *42*, 1562.

(3) Stefanska, A. L.; Cassels, R.; Ready, S. J.; Warr, S. R. SB-2037307 and SB-203208, Two Novel Isoleucyl TRNA Synthetase Inhibitors from a Streptomyces Sp. I. Fermentation, Isolation and Properties. *J. Antibiot. (Tokyo)* **2000**, *53* (4), 357−363.

(4) Houge-Frydrych, C. S. V.; Gilpin, M. L.; Skett, P. W.; Tyler, J. W. SB-203207 and SB-203208, Two Novel Isoleucyl TRNA Synthetase Inhibitors from a Streptomyces Sp. *J. Antibiot. (Tokyo)* **2000**, *53* (4), 364−372.

(5) Banwell, M. G.; Crasto, C. F.; Easton, C. J.; Forrest, A. K.; Karoli, T.; March, D. R.; Mensah, L.; Nairn, M. R.; O'Hanlon, P. J.; Oldham, M. D.; Yue, W. Analogues of SB-203207 as Inhibitors of TRNA Synthetases. *Bioorg. Med. Chem. Lett.* **2000**, *10* (20), 2263−2266.

(6) Crasto, C. F.; Forrest, A. K.; Karoli, T.; March, D. R.; Mensah, L.; O'Hanlon, P. J.; Nairn, M. R.; Oldham, M. D.; Yue, W.; Banwell, M. G.; Easton, C. J. Synthesis and Activity of Analogues of the Isoleucyl TRNA Synthetase Inhibitor SB-203207. *Bioorg. Med. Chem.* **2003**, *11* (13), 2687−2694.

(7) Hager, A.; Vrielink, N.; Hager, D.; Lefranc, J.; Trauner, D. Synthetic approaches towards alkaloids bearing α-tertiaryamines. *Nat. Prod. Rep.* **2016**, *33*, 491.

(8) Hu, Z.; Awakawa, T.; Ma, Z.; Abe, I. Aminoacyl Sulfonamide Assembly in SB-203208 Biosynthesis. *Nat. Commun.* **2019**, *10* (1), 1−10.

(9) Cordell, G. A. Chapter 5 - The Monoterpene Alkaloids. In *The Alkaloids: Chemistry and Biology*; Cordell, G. A., Ed.; Academic Press, 1999; Vol. *52*, pp 261−376.

(10) Kende, A. S.; Liu, K.; Jos Brands, K. M. Total Synthesis of (−)-Altemicidin: A Novel Exploitation of the Potier-Polonovski Rearrangement. *J. Am. Chem. Soc.* **1995**, *117* (42), 10597−10598.

(11) Hirooka, Y.; Ikeuchi, K.; Kawamoto, Y.; Akao, Y.; Furuta, T.; Asakawa, T.; Inai, M.; Wakimoto, T.; Fukuyama, T.; Kan, T. Enantioselective Synthesis of SB-203207. *Org. Lett.* **2014**, *16* (6), 1646−1649.

(12) Banwell, M. G.; Crasto, C. F.; Easton, C. J.; Karoli, T.; March, D. R.; Nairn, M. R.; O'Hanlon, P. J.; Oldham, M. D.; Willis, A. C.; Yue, W. Multi-Component Assembly of the Bicyclic Core Associated with the TRNA Synthetase Inhibitors SB-203207 and SB-203208. Application to the Synthesis of Biologically Active Analogues. *Chem. Commun.* **2001**, No. 21, 2210−2211.

(13) Ohfune, Y.; Shinada, T. Enantio- and Diastereoselective Construction of α,α-Disubstituted α-Amino Acids for the Synthesis of Biologically Active Compounds. *Eur. J. Org. Chem.* **2005**, *2005* (24), 5127−5143.

(14) Nasirova, D. K.; Malkova, A. V.; Polyanskii, K. B.; Yankina, K. Yu.; Amoyaw, P. N.-A.; Kolesnik, I. A.; Kletskov, A. V.; Godovikov, I. A.; Nikitina, E. V.; Zubkov, F. I. Rearrangement of 2-Azanorbornenes to Tetrahydrocyclopenta[c]Pyridines under the Action of Activated Alkynes - A Short Pathway for Construction of the Altemicidin Core. *Tetrahedron Lett.* **2017**, *58* (46), 4384−4387.

(15) Hayakawa, I.; Nagayasu, A.; Sakakura, A. Toward the Synthesis of SB-203207: Construction of Four Contiguous Nitrogen-Containing Stereogenic Centers. *J. Org. Chem.* **2019**, *84* (23), 15614−15623.

(16) Reetz, M. T.; Kayser, F.; Harms, K. Cycloaddition Reactions of Gamma-Amino Alpha, Beta-Didehydro Amino-Acid Esters - a Test Case for the Principle of 1,3-Allylic Strain. *Tetrahedron Lett.* **1992**, *33* (24), 3453−3456.

(17) Kan, T.; Kawamoto, Y.; Asakawa, T.; Furuta, T.; Fukuyama, T. Synthetic Studies on Altemicidin: Stereocontrolled Construction of the Core Framework. *Org. Lett.* **2008**, *10*, 169−171.

(18) Baran, P. S.; Maimone, T. J.; Richter, J. M. Total Synthesis of Marine Natural Products Without Using Protecting Groups. *Nature* **2007**, *446*, 404−408.

(19) Condakes, M. L.; Hung, K.; Harwood, S. J.; Maimone, T. J. Total Syntheses of (−)-Majucin and (−)-Jiadifenoxolane A, Complex Majucin-Type Illicium Sesquiterpenes. *J. Am. Chem. Soc.* **2017**, *139*, 17783−17786.

(20) Hung, K.; Condakes, M. L.; Morikawa, T.; Maimone, T. J. Oxidative Entry into the Illicium Sesquiterpenes: Enantiospecific Synthesis of (+)-Pseudoanisatin. *J. Am. Chem. Soc.* **2016**, *138*, 16616−16619.

(21) Hung, K.; Condakes, M. L.; Novaes, L. F. T.; Harwood, S. J.; Morikawa, T.; Yang, Z.; Maimone, T. J. Development of a Terpene Feedstock-based Oxidative Synthetic Approach to the *Illicium* Sesquiterpenes. *J. Am. Chem. Soc.* **2019**, *141*, 3083.

(22) Harmange Magnani, C. S.; Thach, D. Q.; Haelsig, K. T.; Maimone, T. J. Syntheses of Complex Terpenes from Simple Polyprenyl Precursors. *Acc. Chem. Res.* **2020**, *53*, 949.

(23) Spitzner, D. Product Class 1: Pyridines. *Science of Synthesis* **2005**, *15*, 11.

(24) Kröhnke, F.; Ellegast, K.; Bertram, E. Anlagerungen von Methyl- und Methylen-Ketonen an Pyridiniumbasen. Über Pseudobasen I. *Justus Liebigs Ann. Chem.* **1956**, *600* (3), 176−197.

(25) Comins, D. L.; Higuchi, K.; Young, D. W. Chapter Six - Dihydropyridine Preparation and Application in the Synthesis of Pyridine Derivatives. In *Advances in Heterocyclic Chemistry*; Katritzky, A. R., Ed.; Academic Press, 2013; Vol. *110*, pp 175−235.

(26) Wenkert, E. Alkaloid Synthesis. *Acc. Chem. Res.* **1968**, *1* (3), 78−81.

(27) Bennasar, M. L.; Lavilla, R.; Alvarez, M.; Bosch, J. Addition of Stabilized Carbon Nucleophiles to N-Alkylpyridinium Salts - Applications to Alkaloid Synthesis. *Heterocycles* **1988**, *27* (3), 789−824.

(28) Bosch, J.; Bennasar, M. L.; Zulaica, E.; Feliz, M. Total Synthesis and Stereochemical Reassignment of the Indole Alkaloid Vinoxine. *Tetrahedron Lett.* **1984**, *25* (29), 3119−3122.

(29) Bennasar, M. L.; Vidal, B.; Bosch, J. First Total Synthesis of the Indole Alkaloid Ervitsine. A Straightforward, Biomimetic Approach. *J. Am. Chem. Soc.* **1993**, *115* (12), 5340−5341.

(30) Kröhnke, F. Synthesen mit Hilfe von Pyridiniumsalzen. *Angew. Chem.* **1953**, *65* (24), 605−606.

(31) Bull, J. A.; Mousseau, J. J.; Pelletier, G.; Charette, A. B. Synthesis of Pyridine and Dihydropyridine Derivatives by Regio- and Stereoselective Addition to N-Activated Pyridines. *Chem. Rev.* **2012**, *112* (5), 2642−2713.

(32) Comins, D. L.; Brown, J. D. Regioselective Addition of Titanium Enolates to 1-Acylpyridinium Salts. A Convenient Synthesis of 4-(2-Oxoalkyl)Pyridines. *Tetrahedron Lett.* **1984**, *25* (31), 3297−3300.

https://doi.org/10.1021/jacsau.3c00417
JACS Au 2023, 3, 2883−2893

(33) Comins, D. L.; Hong, H. The Addition of Metallo Enolates to Chiral 1-Acylpyridinium Salts. An Asymmetric Synthesis of (−)-Sedamine. *J. Org. Chem.* **1993**, *58* (19), 5035−5036.
(34) We could install a diazo group at this position using *p*-ABSA, but further chemistry on this derivative did not provide a viable path forward.
(35) Akiba, K.; Nishihara, Y.; Wada, M. Regioselective Synthesis of 4-(2-Oxoalkyl)Pyridines via 1,4-Dihydro-Pyridine Derivatives Using Silyl Enol Ethers and Pyridinium Salts. *Tetrahedron Lett.* **1983**, *24* (47), 5269−5272.
(36) Akiba, K.; Ohtani, A.; Yamamoto, Y. Synthesis of N-Substituted 4-(2-Oxoalkyl)-1,4-Dihydronicotinates and Their Inverse Electron Demand Diels-Alder Reaction with 3,4-Dichlorothiophene 1,1-Dioxide. *J. Org. Chem.* **1986**, *51* (26), 5328−5332.
(37) Yamaguchi, R.; Hatano, B.; Nakayasu, T.; Kozima, S. Triflate Ion-Promoted Addition Reactions of Allylsilane to Quinolines and Isoquinolines Acylated by Chloroformate Esters. *Tetrahedron Lett.* **1997**, *38* (3), 403−406.
(38) Pabel, J.; Hösl, C. E.; Maurus, M.; Ege, M.; Wanner, K. Th. Generation of N-Acylpyridinium Ions from Pivaloyl Chloride and Pyridine Derivatives by Means of Silyl Triflates. *J. Org. Chem.* **2000**, *65* (26), 9272−9275.
(39) Obradors, C.; List, B. Azine Activation via Silylium Catalysis. *J. Am. Chem. Soc.* **2021**, *143* (18), 6817−6822.
(40) Becker, M. R.; Wearing, E. R.; Schindler, C. S. Synthesis of Azetidines via Visible-Light-Mediated Intermolecular [2 + 2] Photocycloadditions. *Nat. Chem.* **2020**, *12* (10), 898−905.
(41) Grigg, R.; Markandu, J. Palladium (II) Catalysed Tandem [2,3]-Sigmatropic Shift-1,3-Dipolar Cycloaddition Processes in Oxime O-Allyl Ethers. *Tetrahedron Lett.* **1991**, *32* (2), 279−282.
(42) We also detected the chlorinated oxime shown below in reactions using DCE at elevated temperatures.

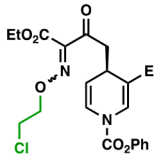

.

(43) Preliminary results indicate the possibility of rendering this synthesis enantioselective using the divergent asymmetric reduction shown below:

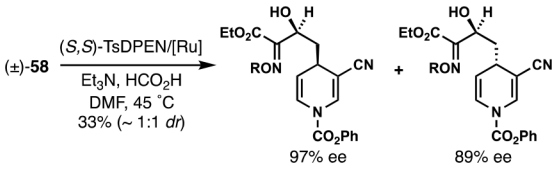

.

(44) For a discussion on proximity-induced cycloadditions that proceed at low temperature, see: Krenske, E. H.; Perry, E. W.; Jerome, S. V.; Maimone, T. J.; Baran, P. S.; Houk, K. N. Why a Proximity-Induced Diels-Alder Reaction Is So Fast. *Org. Lett.* **2012**, *14*, 3016−3019.
(45) DFT calculations were performed on a methyl ester bearing substrate rather than the ethyl ester used in the synthesis.
(46) The calculated free energy barriers in the minor secondary alcohol diastereomeric series were also lower for the (*E*)-configured nitrone isomer by ∼5 kcal mol^{-1} ($\Delta G^{\ddagger}$ = 21.1 vs 26.0 kcal/mol^{-1}).
(47) Amin, J. H.; de Mayo, P. The Irradiation of Aryl Aldoximes. *Tett. Lett.* **1963**, *4*, 1585−1589.
(48) Szostak, M.; Spain, M.; Procter, D. J. Recent Advances in the Chemoselective Reduction of Functional Groups Mediated by Samarium(II) Iodide: A Single Electron Transfer Approach. *Chem. Soc. Rev.* **2013**, *42* (23), 9155−9183.
(49) Faller, J. W.; Brummond, K. M.; Mitasev, B. Hexacarbonylmolybdenum. In *Encyclopedia of Reagents for Organic Synthesis*; Paquette, L., Ed.; John Wiley & Sons: New York, 2006.
(50) Patra, A.; Bandyopadhyay, M.; Mal, D. Mo(CO)6-Promoted Facile Deoxygenation of α,β-Epoxy Ketones and α,β-Epoxy Esters. *Tetrahedron Lett.* **2003**, *44* (11), 2355−2357.
(51) Perez, D.; Greenspoon, N.; Keinan, E. Molybdenum(0)-Catalyzed Reductive Dehalogenation of. Alpha.-Halo Ketones with Phenylsilane. *J. Org. Chem.* **1987**, *52* (25), 5570−5574.
(52) Liu, F.-C.; Sheu, Y.-C.; She, J.-J.; Chang, Y.-C.; Hong, F.-E.; Lee, G.-H.; Peng, S.-M. Syntheses and Characterizations of Group 6 Metal Cyanotrihydroborate Complexes. *J. Organomet. Chem.* **2004**, *689* (3), 544−551.
(53) Pelletier, G.; Bechara, W. S.; Charette, A. B. Controlled and Chemoselective Reduction of Secondary Amides. *J. Am. Chem. Soc.* **2010**, *132* (37), 12817−12819.
(54) Compound **82** was formed as a 1:1 mixture with another separable but spectroscopically distinct compound presumed to be either a rotomer or tautomer. These compounds converge to **84** when coupled with carboxylic acid **83**.
(55) Nisole, C.; Uriac, P.; Huet, J.; Toupet, L. Reactivity of 4-Aminoazetidin-2-Ones: Obtention of Gem-Difunctional Derivatives by N-1-C-4 Cleavage. *J. Chem. Res. (S)* **1991**, No. 8, 204−205.
(56) Earlier attempts to add the sulfonamide side chain to compound **69** using mesyl chloride to activate the carboxylic acid were met with an unexpected rearrangement of the side chain and functionalization of the secondary alcohol as shown below:

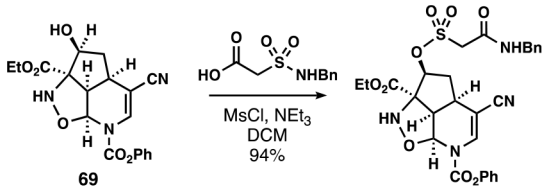

.

(57) Barra, L.; Awakawa, T.; Shirai, K.; Hu, Z.; Bashiri, G.; Abe, I. β-NAD as a Building Block in Natural Product Biosynthesis. *Nature* **2021**, *600* (7890), 754−758.
(58) Barra, L.; Awakawa, T.; Abe, I. Noncanonical Functions of Enzyme Cofactors as Building Blocks in Natural Product Biosynthesis. *JACS Au* **2022**, *2* (9), 1950−1963.
(59) Lee, Y.-H.; Ren, D.; Jeon, B.; Liu, H.-W. *S*-Adenosylmethionine: more than just a methyl donor. *Nat. Prod. Rep.* **2023**, *40*, 1521.
(60) Walsh, C. T.; Moore, B. S. Enzymatic Cascade Reactions in Bio synthesis. *Angew. Chem., Int. Ed.* **2019**, *58* (21), 6846−6879.
(61) Harmange Magnani, C. S.; Maimone, T. J. Dearomative Synthetic Entry into the Altemicidin Alkaloids. *J. Am. Chem. Soc* **2021**, *143*, 7935.
(62) Hetzler, B. E.; Trauner, D.; Lawrence, A. L. Natural product anticipation through synthesis. *Nat. Rev. Chem.* **2022**, *6*, 170−181.

https://doi.org/10.1021/jacsau.3c00417
JACS Au 2023, 3, 2883−2893